Radiology

Impact of in Vivo High-Field-Strength and Ultra-High-Field-Strength MR Imaging on DNA Double-Strand-Break Formation in Human Lymphocytes[1]

Annika Reddig, MS
Mahsa Fatahi, MS
Dirk Roggenbuck, PhD
Jens Ricke, MD
Dirk Reinhold, MD
Oliver Speck, PhD
Björn Friebe, MD

Purpose: To determine the impact of different magnetic field strengths (1, 1.5, 3, and 7 T) and the effect of contrast agent on DNA double-strand–break (DSB) formation in patients undergoing magnetic resonance (MR) imaging.

Materials and Methods: This in vivo study was approved by the local ethics committee, and written informed consent was obtained from each patient. To analyze the level of DNA DSBs, peripheral blood mononuclear cells were isolated from blood samples drawn directly before, as well as 5 minutes and 30 minutes after MR imaging examination. After performing γH2AX immunofluorescence staining, DSBs were quantified with automated digital microscopy. MR group consisted of 43 patients (22 women, 21 men; mean age, 46.1 years; range, 20–77 years) and was further subdivided according to the applied field strength and administration of contrast agent. Additionally, 10 patients undergoing either unenhanced or contrast material–enhanced computed tomography (CT) served as positive control subjects. Statistical analysis was performed with Friedman test.

Results: Whereas DSBs in lymphocytes increased after CT exposure (before MR imaging: 0.14 foci per cell ± 0.05; 5 minutes after: 0.26 foci per cell ± 0.07; 30 minutes after: 0.24 foci per cell ± 0.07; $P \leq .05$), no alterations were observed in patients examined with MR imaging (before MR imaging: 0.13 foci per cell ± 0.02; 5 minutes after: 0.12 foci per cell ± 0.02; 30 minutes after: 0.11 foci per cell ± 0.02; $P > .05$). Differentiated analysis of MR imaging subgroups again revealed no significant changes in γH2AX level.

Conclusion: Analysis of γH2AX foci showed no evidence of DSB induction after MR examination, independent of the applied field strength and administration of gadolinium-based contrast agent.

[1] From the Institute of Molecular and Clinical Immunology (A.R., D. Reinhold); Department of Biomedical Magnetic Resonance (M.F., O.S.); and Department of Radiology and Nuclear Medicine (J.R., B.F.), Otto von Guericke University Magdeburg, Leipziger Str 44, 39120 Magdeburg, Germany; Medipan, Berlin, Germany (D. Roggenbuck); Institute of Biotechnology, Brandenburg University of Technology Cottbus-Senftenberg, Senftenberg, Germany (D. Roggenbuck); Leibniz Institute for Neurobiology, Magdeburg, Germany (O.S.); Center for Behavioral Brain Sciences, Magdeburg, Germany (O.S.); and German Center for Neurodegenerative Disease, Site Magdeburg, Magdeburg, Germany (O.S.).
Received April 5, 2016; revision requested May 13; final revision received June 9; accepted July 6; final version accepted July 20. **Address correspondence to** A.R. (e-mail: *annika.reddig@med.ovgu.de*).

Supported by basic research funding of the Otto von Guericke University Magdeburg, Germany, and by FP7 Marie Curie Actions of the European Commission (FP7-PEOPLE-2012-ITN-316716).

It is well known that ionizing radiation used in x-ray–based imaging, such as computed tomography (CT), can lead to potential carcinogenic damage in human cells and the as low as reasonably achievable, or ALARA, principle is widely accepted (1). Today, the debate is shifting toward magnetic resonance (MR) imaging, which has traditionally been used in children and pregnant women to avoid the use of ionizing radiation. MR imaging is considered to be a safe and powerful diagnostic tool, but the knowledge about possible long-term biologic effects on humans is limited.

In 2013, Fiechter et al reported an induction of DNA double-strand breaks (DSBs) by means of 1.5-T cardiac MR imaging and raised awareness not only in the MR imaging community (2). Contradictory results concerning the genotoxic potential of MR imaging, as well as the development of ultra-high-field-strength MR imagers exceeding a static magnetic field (SMF) of 3 T, demand research that answers whether the growing population of subjects annually examined with clinical or research MR imaging is at any increased mutagenic risk.

One of the most sensitive biomarkers for radiation biodosimetry is γH2AX, a histone protein rapidly phosphorylated after DSB formation (3,4). Immunofluorescence staining allows visualization of individual DSBs as single nuclear γH2AX foci (5).

The aim of our in vivo study was to investigate the impact of different magnetic field strengths and the effect of gadolinium-based contrast agent (GBCA) gadobutrol on γH2AX foci formation in peripheral blood mononuclear cells of patients undergoing MR imaging.

Advances in Knowledge

- There is no evidence ($P > .05$) of DNA double-strand–break induction with unenhanced clinical (1 T, 1.5 T, 3 T) MR imaging (before: 0.11 foci per cell ± 0.02; 5 and 30 minutes after: 0.10 foci per cell ± 0.02) or with gadolinium-based contrast-enhanced (gadobutrol) clinical MR imaging (before: 0.15 foci per cell ± 0.04; 5 and 30 minutes after: 0.13 foci per cell ± 0.04).
- Lymphocytes of patients undergoing unenhanced 7-T ultra-high-field-strength MR imaging showed no significant changes in γH2AX level before and after examination (before: 0.12 foci per cell ± 0.04; 5 and 30 minutes after: 0.11 foci per cell ± 0.04).

Materials and Methods

Study Design and Participants

All patients who agreed to participate in this study provided written informed consent. The study was performed in accordance with the Declaration of Helsinki and was approved by the local ethics committee (RAD244 DSB-MRT).

Patients undergoing either MR imaging (n = 43) or CT (n = 10) were recruited for this study between April 2014 and October 2015. Eligible participants were adults aged 18–80 years. Scheduled patients were excluded if they had undergone x-ray–based or nuclear imaging within the past 3 days, had undergone radiation therapy or chemotherapy, or if they were previously diagnosed with lymphoma or leukemia. Further, subjects examined with contrast material–enhanced MR imaging were only included when gadobutrol was administered.

Procedures

Different MR imagers covering the most common SMFs used in clinics (1 T, 1.5 T, 3 T) and for the first time a 7-T ultra-high-field-strength MR system, currently only allowed for research purposes, were included for in vivo genotoxicity analysis. Patients undergoing x-ray–based CT served as positive control subjects. Patients were assigned to nine groups according to the imaging procedure they underwent: 1-T MR imaging without contrast agent (n = 5), 1-T MR imaging with contrast agent (n = 5), 1.5-T MR imaging without contrast agent (n = 5), 1.5-T MR imaging with contrast agent (n = 5), 3-T MR imaging without contrast agent (n = 5), 3-T MR imaging with contrast agent (n = 5), 7-T MR imaging without contrast agent (n = 13), CT without contrast agent (n = 5), and CT with contrast agent (n = 5). Diagnostic MR imaging was conducted with imagers differing in their SMF strength, with use of 1-T (Panorama; Philips Healthcare, Best, the Netherlands), 1.5-T (Intera; Philips Healthcare), 3-T (Achieva; Philips Healthcare), and 7-T (Siemens Healthcare, Erlangen, Germany) MR systems. Besides unenhanced routine MR imaging, subgroups additionally received 0.1 mmol per kilogram of body weight of the GBCA gadobutrol (Gd-DO3A-butrol, Gadovist; Bayer Healthcare, Leverkusen, Germany) during 1–3 T MR imaging. As positive control subjects for ionizing radiation–induced

Implication for Patient Care

- In contrast to CT, high-field-strength and ultra-high-field-strength MR imaging, as well as administration of contrast agent gadobutrol, did not induce detectable alterations in γH2AX level, confirming MR imaging as safe imaging technique.

Published online before print
10.1148/radiol.2016160794 **Content codes:** PH MR

Radiology 2017; 282:782–789

Abbreviations:
DSB = double-strand break
GBCA = gadolinium-based contrast agent
SAR = specific absorption rate
SMF = static magnetic field

Author contributions:
Guarantor of integrity of entire study, A.R.; study concepts/study design or data acquisition or data analysis/interpretation, all authors; manuscript drafting or manuscript revision for important intellectual content, all authors; approval of final version of submitted manuscript, all authors; agrees to ensure any questions related to the work are appropriately resolved, all authors; literature research, A.R., M.F., J.R., B.F.; clinical studies, A.R., M.F., B.F.; experimental studies, A.R., M.F., D. Roggenbuck, D. Reinhold, B.F.; statistical analysis, A.R., M.F., O.S., B.F.; and manuscript editing, all authors

Conflicts of interest are listed at the end of this article.

γH2AX foci, patients undergoing either unenhanced or iodine-based contrast-enhanced (80–120 mL Imeron 300; Bracco Imaging, Milan, Italy) CT (Aquilion Prime, Toshiba Medical Systems, Tustin, Calif; or Somatom Definition AS, Siemens Healthcare, Erlangen, Germany, respectively) were enrolled.

Venous peripheral blood was drawn from each patient into heparinized vacuum tubes directly before imaging as well as 5 minutes and 30 minutes after examination. Each sample was processed immediately after withdrawal, and peripheral blood mononuclear cells were isolated by means of density-gradient centrifugation. Separated cells were stored on ice at a density of 1×10^6 cells/mL until cells from the remaining time points were purified. Afterward, γH2AX staining was performed as described in detail previously (6). In brief, peripheral blood mononuclear cells were washed in Dulbecco's phosphate buffered saline (Biochrom, Berlin, Germany), pipetted onto silanized glass slides (Medipan, Berlin/Dahlewitz, Germany), fixed in 1% paraformaldehyde, and subsequently permeabilized in 0.2% Triton X-100 (Sigma-Aldrich, Taufkirchen, Germany). After blocking (phosphate buffered saline containing 1% bovine serum albumin, 30 minutes), anti-phospho-histone H2AX mouse monoclonal immunoglobulin G primary antibody (clone JBW301; Millipore, Schwalbach, Germany) at a 1:2000 dilution was added for 1 hour at room temperature. Following a washing cycle in blocking buffer, cells were incubated for 1 hour with a polyclonal goat antimouse immunoglobulin G antibody (Alexa Fluor 488 conjugate; Lifetechnologies, Darmstadt, Germany, catalog number A11001) at a 1:2000 dilution. To reduce operator bias, we applied automated digital microscopy analysis for γH2AX foci quantification. Stained slides were covered with 4',6-diamidino-2-phenylindole–containing mounting medium (Medipan, Berlin/Dahlewitz, Germany), and γH2AX analysis of 200–300 cells per sample was performed within 24 hours by using a fully automated digital microscopy system (AKLIDES; Medipan) (6,7).

Statistical Analysis

Statistical analysis was performed by using GraphPad Prism software, version 5.01 (Graph Pad Software, La Jolla, Calif), and data in text and figures are displayed as mean ± standard error of the mean. Significance levels were calculated by means of Friedman tests with 95% confidence interval ($\alpha = .05$) followed by Dunns posthoc tests. Comparison was only performed within the same group between initial values and corresponding values at different times after exposure. No mathematical correction for multiple comparisons was made, increasing the probability to falsely detect a DSB-inducing effect that is not present. To compare differences between MR and CT exposure, normalized data were analyzed by a Mann-Whitney test at 5 minutes and 30 minutes after exposure. Minimal detectable effect size was calculated according to Cohen (8) by performing a power analysis for nonparametric tests for the given α of .05, standard deviation, number of patients, and power of 0.8 by using XLSTAT for MS Excel (version 2015, Microsoft, Redmond, Wash). Significance was defined as $P \leq .05$.

Results

In this study, 43 patients (mean age, 46.1 years [range, 20–77 years]; 22 women with mean age of 44.5 years [range: 26–71 years] and 21 men with mean age of 47.7 years [range: 20–77 years]) were examined with MR imaging. Demographic characteristics of the patients assigned to the different MR imaging subgroups, the type of imaging, and the mean radiofrequency field exposure are displayed in the Table. For estimation and quantification of the exposed radiofrequency field in different MR protocols, the mean applied whole-body SAR for each protocol used is listed, as well as a standardized energy dose in joules per kilogram (whole-body SAR multiplied by total exposure time). Further, 10 patients examined at CT (mean age, 64.6 years [range, 48–80 years]; three women with a mean age 63.0 years [range, 51–77 years] and seven men with a mean age of 65.3 years [range, 48–80 years]) served as positive control subjects. Dependent on the additional injection of iodinated contrast agent, patients undergoing CT were also classified into unenhanced and enhanced group (two thorax and three abdominal CT examinations per CT subgroup).

The mean level of initial γH2AX foci (before examination) in lymphocytes from all 53 patients was 0.13 foci per cell ± 0.02. No significant difference ($P = .699$) in basal DSB level was observed between male and female subjects. Combined results of all 43 subjects within the MR groups revealed a mean baseline level of 0.13 foci per cell ± 0.02 (before MR imaging). No significant changes were determined after MR exposure (5 minutes after: 0.12 foci per cell ± 0.02; 30 minutes after: 0.11 foci per cell ± 0.02), as shown in Figure 1a. In contrast, CT examination led to a significant induction of DNA DSBs, increasing from a mean γH2AX baseline level of 0.14 foci per cell ± 0.05 to 0.26 foci per cell ± 0.07 5 minutes after CT and 0.24 foci per cell ± 0.07 30 minutes after CT.

Unlike studies where only healthy volunteers were enrolled (6,9), heterogeneity of initial γH2AX values increased in our in vivo study, ranging from 0.01 to 0.58 foci per cell. This spread in individual baseline DSBs led to high standard deviations. To account for individual differences and not to underestimate personal risk, we normalized the results obtained 5 and 30 minutes after examination to the individual DSB values at baseline (Fig 1b). Thereby the coefficient of variation for the MR group was reduced by more than 50%. Again, relative results revealed no changes within the MR group (before MR imaging: 1.00; 5 minutes: 0.94 ± 0.07; 30 minutes: 0.96 ± 0.06), whereas γH2AX foci increased significantly ($P \leq .05$) after CT examination (5 minutes: 4.00 ± 1.13; 30 minutes: 2.52 ± 0.49). In comparison to absolute values, CT results exhibited even

Estimated Absorbed Energy according to Different MR Protocols and Patient Demographics

Protocol	Mean Whole-Body SAR (w/kg)	Exposure Time (sec)	SED (J/kg)	No. of Patients	No. of Women	No. of Men	Age (y)*
1-T MR imaging without contrast agent							
Shoulder	0.4	2070	828	5	3	2	32.8 ± 11.7
1-T MR imaging with contrast agent							
Cardiac	0.3	605	182	5	3	2	39.8 ± 17.2
1.5-T MR imaging without contrast agent							
Abdominal	1.4	755	1057	3	3	0	46.7 ± 7.0
Knee	2.1	1345	2825	1	1	0	55
Thorax	2.4	679	1630	1	1	0	26
1.5-T MR imaging with contrast agent							
Lumbar spine	2.6	1656	4306	1	0	1	45
Lung	2.0	679	1358	1	0	1	70
Pancreas	2.0	1409	2818	2	0	2	64.5 ± 17.7
Pelvis	1.4	761	1065	1	1	0	28
3-T MR imaging without contrast agent							
Ankle	0.9	1439	1295	1	1	0	60
Cervical spine	1.3	2038	2649	1	1	0	37
Knee	1.1	1227	1350	3	1	2	43.0 ± 2.0
3-T MR imaging with contrast agent							
Lumbar spine	1.3	1188	1544	1	0	1	77
Pelvis	1.1	1673	1840	2	0	2	60.0 ± 14.1
Prostate	1.2	1432	1718	1	0	1	71
Rectum	1.2	1861	2233	1	1	0	72
7-T MR imaging without contrast agent							
Knee	0.2	1982	396	13	6	7	43.2 ± 13.5

Note.—SAR = specific absorption rate, SED = standardized energy dose (SED = mean whole-body SAR × exposure time).

* Where applicable, data are means ± standard deviation.

stronger differences in relative γH2AX level due to the high range of individual baseline levels.

Differentiated analysis of subgroups, classified according to the applied SMF and the administration of GBCA, also showed no significant change in the amounts of DSBs before and after MR examination (Fig 2a). In each group, a minimum of five subjects (7 T: $n = 13$) were analyzed. Compared with unenhanced high-field-strength (1-, 1.5-, 3-T) MR imaging (before imaging: 0.11 foci per cell ± 0.02; 5 minutes after: 0.10 foci per cell ± 0.02; 30 minutes after: 0.10 foci per cell ± 0.02), there was no evidence that GBCA-enhanced high-field-strength MR imaging (before imaging: 0.15 foci per cell ± 0.04; 5 minutes after: 0.13 foci per cell ± 0.04; 30 minutes after: 0.13 foci per cell ± 0.04) or unenhanced ultra-high-field-strength 7-T MR imaging (before imaging: 0.12 foci per cell ± 0.04; 5 minutes after: 0.11 foci per cell ± 0.04; 30 minutes after: 0.11 foci per cell ± 0.04) led to an increase of γH2AX foci. In the unenhanced CT group, the level of DSBs increased from initially 0.18 foci per cell ± 0.08 to 0.21 foci per cell ± 0.10 (5 minutes after) and 0.27 foci per cell ± 0.12 ($P \leq .05$) (30 minutes after) and after CT examination combined with iodinated contrast agent from initially 0.10 foci per cell ± 0.05 (before imaging) to 0.32 foci per cell ± 0.10 ($P \leq .05$) (5 minutes after) and 0.21 foci per cell ± 0.08 (30 minutes after).

Diagrams displaying the normalized data (Fig 2b) again revealed no changes in relative DSB levels after MR imaging, but an increase after unenhanced CT (5 minutes after: 2.22 ± 0.88; 30 minutes after: 2.27 ± 0.51, $P \leq .05$) and contrast-enhanced CT (5 minutes after: 5.79 ± 1.83, $P \leq .05$; 30 minutes after: 2.77 ± 0.88).

To exclude heterogeneity among different MR imaging groups, stratified analyses of normalized data were conducted. The results showed that neither the applied field strength ($P = .392$) nor administration of GBCA ($P = .317$) affected significantly the γH2AX value determined 5 minutes and 30 minutes after imaging. Although the total number of subjects is high, each subgroup for this analysis contained only five patients, potentially limiting the sensitivity of the study. Comparison of normalized data between the MR imaging and CT group revealed significant differences in the level of induced γH2AX foci at 5 minutes ($P < .0001$) and 30 minutes ($P = .0002$) after exposure (Fig 1b).

Since no significant changes in γH2AX foci values after MR imaging were found, we additionally performed a reverse power analysis to state how high a potentially undetected effect of induced γH2AX foci may be. Reverse power analysis from all normalized MR data revealed a minimal detectable effect size of 0.396 and changes of more than 39.6% should have been detected. This equals a change of more than 0.05 foci referred to the mean baseline level.

Discussion

The results of our in vivo study indicate that neither MR examination alone (1 T, 1.5 T, 3 T, or 7 T) nor addition of

GBCA lead to a detectable induction of DNA DSBs in peripheral blood mononuclear cells. For standardized assessment of γH2AX foci, nuclei were evaluated by automated image analysis.

Whereas different studies consistently reported influences of (ultra)-high-field-strength MR imaging on sensory perception of patients, such as vertigo or metallic taste (10,11), no clear conclusion about genotoxic effects can be drawn so far. Within the past years, different in vitro and in vivo studies analyzed the impact of MR imaging on DNA integrity in human lymphocytes but reported contradictory results. Some observed an increase in comet formation by performing alkaline single-cell gel electrophoresis, an enhanced number of micronuclei or an increase in DNA DSBs detected with

Figure 1

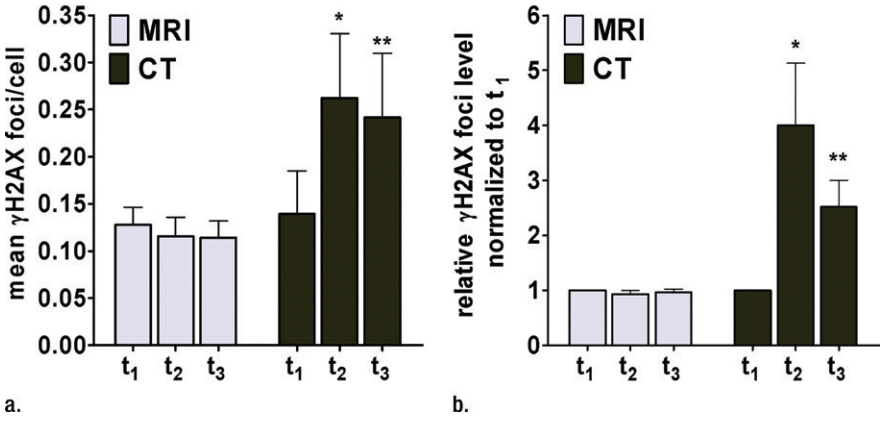

Figure 1: **(a)** Bar graph shows the mean with standard error of the mean of γH2AX foci per cell assessed in lymphocytes before *(t_1)* and 5 minutes *(t_2)* and 30 minutes *(t_3)* after in vivo MR imaging (43 subjects) or CT (10 subjects) exposure. **(b)** Bar graph shows the mean with standard error of the mean of normalized γH2AX values, depicting the relative increase in mean γH2AX foci per cell after MR or CT examination in relation to the individual baseline value before the imaging. ** = $P \leq .01$, * = $P \leq .05$.

Figure 2

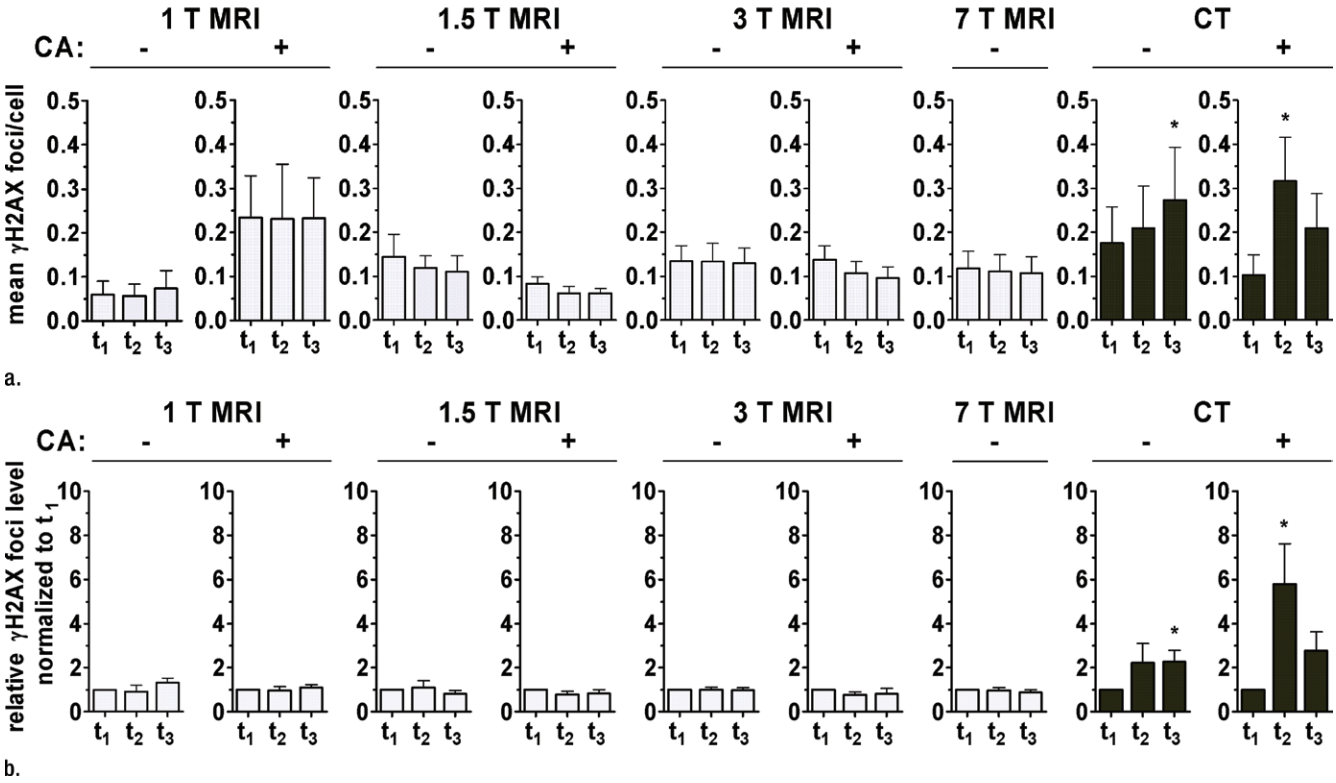

Figure 2: Bar graphs show γH2AX foci per cell assessed in lymphocytes before *(t_1)* and 5 minutes *(t_2)* and 30 minutes *(t_3)* after in vivo MR imaging or CT exposure. Combined data of MR and CT groups shown in Figure 1 were further subdivided according to SMF of the MR imager (1 T, 1.5 T, 3 T, and 7 T) and administration of contrast agent *(CA)*. The mean with standard error of the mean of five patients per condition (7 T: $n = 13$) is displayed for each time point. Graphs show **(a)** the absolute number of γH2AX foci per cell and **(b)** the relative increase in γH2AX level, normalized to the individual baseline value before the imaging. * = $P \leq .05$.

γH2AX analysis (2,12–14). In contrast, different studies did not find such effects induced by MR imaging (6,15,16) or observed an enhanced DNA damage only when a contrast agent was administered (17). Due to variations in the experimental settings, induced energy deposits, and/or applied analysis methods, direct comparison of these studies and their outcomes is difficult. The results published between 2007 and 2013 are discussed in a recent review (18). Especially the study by Fiechter et al raised attention (2). The authors reported an increase in DNA DSBs using γH2AX microscopy and flow cytometry analysis of lymphocytes isolated from 20 patients before and after contrast-enhanced 1.5-T cardiac MR imaging. Findings and limitations of this study were controversially discussed by others (19,20), also resulting in similar investigations and repetitions (6,14,16).

In 2015 two additional reports were published, again evaluating γH2AX formation in lymphocytes isolated before and after 1.5 T cardiac MR imaging. Brand et al (16) investigated the effects of three different cardiac MR imaging protocols, all combined with GBCA. Microscopy analysis of lymphocytes from 45 patients showed no significant changes in DSB levels before (mean, 0.116 foci per cell ± 0.019) and 5 minutes after (mean, 0.117 foci per cell ± 0.019) MR imaging. Lancellotti et al (14), enrolling 20 healthy male participants for noncontrast-enhanced cardiac MR imaging, studied the DSB induction, as well as blood cell counts and activation. Whereas flow cytometric measurements of different T-cell subsets and the whole T-cell population showed no changes in γH2AX level 1 and 2 hours after MR exposure, the authors stated a significant increase in the amount of DSBs within the whole T-cell population 2 days and 1 month after cardiac MR imaging. However, the described increase in γH2AX level 2 days after cardiac MR imaging only occurred in a few subjects, and a high interindividual variation was observed in subjects 1 month after cardiac MR imaging. The reported correlation between the γH2AX values 1 month after exposure and the initial SAR is intriguing but cannot be extrapolated, for example, to no exposure, where a negative number of γH2AX is predicted. Further, sufficient control subjects were not included, and thus it is difficult to judge whether the observed increase in γH2AX fluorescence intensity reflects a specific MR-related effect (21). Long-term or delayed effects of MR imaging exposure were not explicitly investigated in our study. A recent publication by Fatahi et al (9) compared a control group with frequently exposed participants, who were exposed to 7-T MR imaging for up to 175 hours within 1 year. That study revealed no differences in DNA integrity (γH2AX foci, micronuclei), supporting the hypothesis that no long-term or delayed effects are induced (9).

In our in vivo study, we investigated different MR examinations and their impact on DNA DSB formation. Thereby, we attempted to reveal a potential hazardous effect of GBCA and the impact of the electromagnetic fields applied in MR imaging on subjects in daily routine or research. Radiofrequency field energy deposition can be determined by SAR. Higher SMF usually requires the use of more powerful radiofrequency fields and therefore increased SAR, which always has to stay within the strict regulatory guidelines of the International Electrotechnical Commission (IEC) (22). According to the IEC guidelines, the whole-body SAR must not exceed 4 W/kg in first-level operation mode averaged over 15 minutes. With adjustment of methods and sequence parameters, SAR is thus often similar, regardless of the field strength. Because of this fact, MR groups were not classified according to specific SAR and/or standardized energy dose but according to the SMF within our study. Of notice is the fact that at higher field strengths, whole-body SAR can even be lower than at lower field strengths since the local SAR limit is usually reached earlier than the whole-body SAR limit and because local transmit coils are used.

Our results revealed no induction of DSBs by MR imaging irrespective of the field strength and contrast material enhancement. For combined MR group, a minimal detectable effect size of 0.396 (± 39.6%) was calculated with reverse power analysis. In comparison, Fiechter et al reported a significant change in quantified γH2AX foci from initially 0.066 to 0.190 foci per cell (median values) after MR imaging, displaying an increase of 0.124 foci (188%) (2).

Whereas there seems to be a causal link between enhanced DNA lesions and administration of iodinated contrast agent during CT (23,24), little is known about the genotoxic impact of GBCAs in MR imaging. An in vitro study by Cho et al indicated a dose- and time-dependent genotoxic effect in gadolinium (III)-treated ($GdCl_3$) lymphocytes, which increased when combined with extremely low frequency electromagnetic field (25). Previous studies also demonstrated cytotoxic effects caused by free gadolinium (26). To evade high toxicity of free Gd^{3+} ions, gadolinium is administered in MR imaging contrast agents as chelated compound. However, dechelation of one commercially available MR imaging contrast agent (gadodiamide [Omniscan]; Amersham Health, Oslo, Norway) under simulated in vivo conditions was described by Robic et al (27). An in vivo study by Yildiz et al (17), which analyzed lymphocytes of 28 subjects after 1.5-T hypophysial MR imaging, reported a slight increase in DNA damage by alkaline comet assay after noncontrast-enhanced MR imaging, which significantly increased after GBCA (Omniscan) was used. A different contrast medium was administered in cardiac MR imaging studies by Fiechter et al (2) (gadobutrol) and Brand et al (gadobutrol or gadoterate meglumine [Dotarem]; Guerbet, Roissy, France) (16). Gadobutrol was also injected during contrast-enhanced MR imaging in our in vivo study. Here, comparison of the unenhanced and contrast-enhanced groups indicated no induction of DSBs in any MR group when related to initial values. As a limitation, one has to take into account that in our study gadobutrol (Gadovist) was used only to keep the groups as homogeneous as possible. Potential effects caused by other GBCAs cannot be excluded. Only large-scale

studies investigating a wide spectrum of currently applied contrast agents under different in vitro and in vivo conditions may reduce uncertainties about an additional genotoxic effect of GBCA used in MR imaging.

In our in vivo study, patients examined with CT in combination with iodinated contrast agents revealed a stronger increase in γH2AX foci 5 minutes after exposure compared with patients examined with CT only. Here, CT patients served as positive control subjects for the detection methods and demonstrated its high sensitivity. To specifically examine potential additive or synergistic effects induced by iodinated contrast medium during CT, more patients as well as different normalization steps need to be included, considering individual baseline level, radiation dose, and in vitro–determined repair capacity, as shown by Grudzenski et al (23).

The results of our in vivo study are based on γH2AX analysis, one of the most sensitive assays for detecting DSBs. Still, some questions about the genotoxic effect of MR imaging remain. Whether or not MR imaging induces oxidative stress or different types of DNA lesions in the short or long term still needs to be addressed in future studies. In the past, the impact of MR imaging was preferably studied in differentiated quiescent lymphocytes, but little is known about a potential genotoxic effect on, for example, highly proliferative human hematopoietic stem/progenitor cells or on cells from individuals carrying deficiencies in DNA damage repair mechanisms.

In conclusion, automated γH2AX foci quantification did not show evidence of increased DNA DSBs after unenhanced or contrast-enhanced in vivo MR imaging at any investigated MR condition, including MR systems with different SMF strengths (1 T, 1.5 T, 3 T, and 7 T). Although additional aspects need to be investigated, if one regards DSBs as one of the most deleterious types of DNA damage, our results are contrary to those of reports describing a potential carcinogenic effect of MR imaging and thus strengthen the acceptance of MR imaging as a safe imaging tool. However, future studies will have to include broader analysis methods that search for different genotoxicity and cytotoxicity markers to exclude potential hazardous biologic effects of MR imaging in even larger cohorts. Until then, according to the precautionary principle, an appropriate use of MR imaging techniques should be ensured.

Disclosures of Conflicts of Interest: A.R. disclosed no relevant relationships. **M.F.** disclosed no relevant relationships. **D.Roggenbuck** Activities related to the present article: disclosed no relevant relationships. Activities not related to the present article: is a shareholder of Medipan and has a patent PCT/EP2012/06499, US 8,835,122, AU11168799.2 issued. Other relationships: disclosed no relevant relationships. **J.R.** disclosed no relevant relationships. **D. Reinhold** disclosed no relevant relationships. **O.S.** Activities related to the present article: disclosed no relevant relationships. Activities not related to the present article: grants from European Commission and from Siemens Healthcare. Other relationships: disclosed no relevant relationships. **B.F.** disclosed no relevant relationships.

References

1. Hendee WR, Edwards FM. ALARA and an integrated approach to radiation protection. Semin Nucl Med 1986;16(2):142–150.
2. Fiechter M, Stehli J, Fuchs TA, Dougoud S, Gaemperli O, Kaufmann PA. Impact of cardiac magnetic resonance imaging on human lymphocyte DNA integrity. Eur Heart J 2013;34(30):2340–2345.
3. Redon CE, Nakamura AJ, Martin OA, Parekh PR, Weyemi US, Bonner WM. Recent developments in the use of γ-H2AX as a quantitative DNA double-strand break biomarker. Aging (Albany, NY) 2011;3(2):168–174.
4. Ivashkevich A, Redon CE, Nakamura AJ, Martin RF, Martin OA. Use of the γ-H2AX assay to monitor DNA damage and repair in translational cancer research. Cancer Lett 2012;327(1-2):123–133.
5. Bonner WM, Redon CE, Dickey JS, et al. GammaH2AX and cancer. Nat Rev Cancer 2008;8(12):957–967.
6. Reddig A, Fatahi M, Friebe B, et al. Analysis of DNA double-strand breaks and cytotoxicity after 7 Tesla magnetic resonance imaging of isolated human lymphocytes. PLoS One 2015;10(7):e0132702.
7. Willitzki A, Lorenz S, Hiemann R, et al. Fully automated analysis of chemically induced γH2AX foci in human peripheral blood mononuclear cells by indirect immunofluorescence. Cytometry A 2013;83(11):1017–1026.
8. Cohen J. Statistical power analysis. Curr Dir Psychol Sci 1992;1(3):98–101.
9. Fatahi M, Reddig A, Vijayalaxmi, et al. DNA double-strand breaks and micronuclei in human blood lymphocytes after repeated whole body exposures to 7T magnetic resonance imaging. Neuroimage 2016;133:288–293.
10. Friebe B, Wollrab A, Thormann M, et al. Sensory perceptions of individuals exposed to the static field of a 7T MRI: a controlled blinded study. J Magn Reson Imaging 2015;41(6):1675–1681.
11. Heinrich A, Szostek A, Meyer P, et al. Cognition and sensation in very high static magnetic fields: a randomized case-crossover study with different field strengths. Radiology 2013;266(1):236–245.
12. Simi S, Ballardin M, Casella M, et al. Is the genotoxic effect of magnetic resonance negligible? low persistence of micronucleus frequency in lymphocytes of individuals after cardiac scan. Mutat Res 2008;645(1-2):39–43.
13. Lee JW, Kim MS, Kim YJ, Choi YJ, Lee Y, Chung HW. Genotoxic effects of 3 T magnetic resonance imaging in cultured human lymphocytes. Bioelectromagnetics 2011;32(7):535–542.
14. Lancellotti P, Nchimi A, Delierneux C, et al. Biological effects of cardiac magnetic resonance on human blood cells. Circ Cardiovasc Imaging 2015;8(9):e003697.
15. Schwenzer NF, Bantleon R, Maurer B, et al. Detection of DNA double-strand breaks using gammaH2AX after MRI exposure at 3 Tesla: an in vitro study. J Magn Reson Imaging 2007;26(5):1308–1314.
16. Brand M, Ellmann S, Sommer M, et al. Influence of cardiac MR imaging on DNA double-strand breaks in human blood lymphocytes. Radiology 2015;277(2):406–412.
17. Yildiz S, Cece H, Kaya I, et al. Impact of contrast enhanced MRI on lymphocyte DNA damage and serum visfatin level. Clin Biochem 2011;44(12):975–979.
18. Vijayalaxmi FM, Fatahi M, Speck O. Magnetic resonance imaging (MRI): a review of genetic damage investigations. Mutat Res Rev Mutat Res 2015;764:51–63.
19. Knuuti J, Saraste A, Kallio M, Minn H. Is cardiac magnetic resonance imaging causing DNA damage? Eur Heart J 2013;34(30):2337–2339.
20. Berrington de Gonzalez A, Kleinerman RA, McAreavey D, Rajaraman P. Cardiac MR

imaging and the specter of double-strand breaks. Radiology 2015;277(2):329–331.

21. Vijayalaxmi MF, Scarfi MR, Fatahi M, Reddig A, Reinhold D, Speck O. Letter by Vijayalaxmi et al regarding article, "Biological Effects of Cardiac Magnetic Resonance on Human Blood Cells" by Lancellotti et al. http://intl-circimaging.ahajournals.org/content/8/9/e003697/reply. Published November 12, 2015. Accessed December 12, 2015.

22. International Electrotechnical Commission. IEC 60601. Medical electrical equipment—Part 2-33: Particular requirements for the basic safety and essential performance of magnetic resonance equipment for medical diagnosis. Geneva, Switzerland: International Electrotechnical Commission, 2015.

23. Grudzenski S, Kuefner MA, Heckmann MB, Uder M, Löbrich M. Contrast medium-enhanced radiation damage caused by CT examinations. Radiology 2009;253(3):706–714.

24. Piechowiak EI, Peter JF, Kleb B, Klose KJ, Heverhagen JT. Intravenous iodinated contrast agents amplify DNA radiation damage at CT. Radiology 2015;275(3):692–697.

25. Cho S, Lee Y, Lee S, Choi YJ, Chung HW. Enhanced cytotoxic and genotoxic effects of gadolinium following ELF-EMF irradiation in human lymphocytes. Drug Chem Toxicol 2014;37(4):440–447.

26. Yongxing W, Xiaorong W, Zichun H. Genotoxicity of lanthanum (III) and gadolinium (III) in human peripheral blood lymphocytes. Bull Environ Contam Toxicol 2000;64(4):611–616.

27. Robic C, Catoen S, De Goltstein MC, Idée JM, Port M. The role of phosphate on Omniscan(®) dechelation: an in vitro relaxivity study at pH 7. Biometals 2011;24(4):759–768.